Negative interactions and virulence differences drive the dynamics in multispecies bacterial infections

Schmitz, Désirée A ; Allen, Richard C ; Kümmerli, Rolf

DOI: https://doi.org/10.1098/rspb.2023.1119

PROCEEDINGS B

royalsocietypublishing.org/journal/rspb

Research

Cite this article: Schmitz DA, Allen RC, Kümmerli R. 2023 Negative interactions and virulence differences drive the dynamics in multispecies bacterial infections. *Proc. R. Soc. B* **290**: 20231119.
https://doi.org/10.1098/rspb.2023.1119

Received: 19 May 2023
Accepted: 27 June 2023

Subject Category:
Ecology

Subject Areas:
microbiology, ecology

Keywords:
multispecies bacterial infections, opportunistic human pathogens, virulence, microbial interactions, microbe–host interactions, *Galleria mellonella*

Authors for correspondence:
Désirée A. Schmitz
e-mail: desiree.schmitz@uzh.ch
Rolf Kümmerli
e-mail: rolf.kuemmerli@uzh.ch

Electronic supplementary material is available online at https://doi.org/10.6084/m9.figshare.c.6729983.

THE ROYAL SOCIETY PUBLISHING

Negative interactions and virulence differences drive the dynamics in multispecies bacterial infections

Désirée A. Schmitz, Richard C. Allen and Rolf Kümmerli

Department of Quantitative Biomedicine, University of Zurich, Zurich, Switzerland

DAS, 0000-0003-1779-9309; RCA, 0000-0001-6012-7888; RK, 0000-0003-4084-6679

Bacterial infections are often polymicrobial, leading to intricate pathogen–pathogen and pathogen–host interactions. There is increasing interest in studying the molecular basis of pathogen interactions and how such mechanisms impact host morbidity. However, much less is known about the ecological dynamics between pathogens and how they affect virulence and host survival. Here we address these open issues by co-infecting larvae of the insect model host *Galleria mellonella* with one, two, three or four bacterial species, all of which are opportunistic human pathogens. We found that host mortality was always determined by the most virulent species regardless of the number of species and pathogen combinations injected. In certain combinations, the more virulent pathogen simply outgrew the less virulent pathogen. In other combinations, we found evidence for negative interactions between pathogens inside the host, whereby the more virulent pathogen typically won a competition. Taken together, our findings reveal positive associations between a pathogen's growth inside the host, its competitiveness towards other pathogens and its virulence. Beyond being generalizable across species combinations, our findings predict that treatments against polymicrobial infections should first target the most virulent species to reduce host morbidity, a prediction we validated experimentally.

1. Introduction

Research over the past decades has revealed that many bacterial infections are polymicrobial [1–4], with four to six different bacterial species commonly being present in infections [5,6]. This can lead to complicated pathogen–pathogen and pathogen–host interactions. The ecological interactions between pathogens can range from competition through commensalism to cooperation, and such interactions can have consequences for the host [7]. For example, mutually beneficial cross-feeding between a human commensal bacterium and a pathogen was shown to increase the virulence of the latter, thus exacerbating host morbidity [8]. Competition can also enhance virulence as revealed for the pathogen *Pseudomonas aeruginosa*, which increases the production of the toxin pyocyanin thereby harming both its competitor *Staphylococcus aureus* and host tissue [9]. Interaction patterns can become even more complex in chronic infections, where (co-)evolution can occur between pathogens and between pathogens and the host [10–15]. There is increasing awareness that such eco-evolutionary dynamics affect host health and are important to consider in the context of treatment options [7].

For this reason, research on interactions between pathogenic bacteria has flourished in recent years. For example, there is a wealth of work on interactions between *P. aeruginosa and S. aureus*, two of the most troublesome nosocomial pathogens [16–18]. This research, often carried out *in vitro*, has successfully identified molecular mechanisms of pathogen interactions and evolutionary patterns of how pathogens adapt to one another. However, we know much less about pathogen–pathogen interactions within hosts and how interactions drive virulence. Moreover, it is often unclear whether insights from a particular

pathogen pair are generalizable and hold for other pathogen and strain combinations [19].

Here, we aim to tackle these questions by studying bacterial interactions between four different opportunistic human pathogens in an insect host, the larvae of the greater wax moth *Galleria mellonella*. This model host is suitable for our purpose because it allows for relatively high-throughput experiments where many different pathogen combinations can be tested, and well-defined doses of pathogens can be injected into a larva. Moreover, *G. mellonella* has an innate immune system that resembles the vertebrate innate immune response and lives approximately at human body temperature, which makes it an excellent model organism to study human bacterial pathogenesis [20–23]. Regarding the pathogens, our aim was to choose four gram-negative bacterial species that exhibit different levels of virulence in order to test whether generalizable patterns of host survival and pathogen interactions arise across a spectrum of pathogens. We picked the following four opportunistic human pathogens. *Pseudomonas aeruginosa* (P) is a species of high clinical relevance that causes both community- and hospital-acquired infections including skin and wound infections, urinary tract infections, bloodstream infections and pneumonias [24,25]. *Burkholderia cenocepacia* (B) causes chronic lung infections in immunocompromised patients, e.g. suffering from cystic fibrosis [26]. *Klebsiella michiganensis* (K) belongs to the *K. oxytoca* complex [27], which are human pathogens that lead to healthcare-associated infections as well as to a variety of infections such as diarrhea, bacteremia and meningitis [28–30]. *Cronobacter sakazakii* (C) can also cause bacteraemia and meningitis as well as necrotizing enterocolitis and brain abscess/lesions [31]. While some of these pathogens can be found together—P and B in lung infections of cystic fibrosis patients [4,32,33] and P and K in burn wound infections [34,35]—co-occurrence for other combinations is rarer. Thus, our model reflects a scenario where different opportunistic pathogens co-incidentally infect the same host without any prior interaction history or coevolution between the co-infecting pathogens. Such a scenario reflects the starting point of many acute and chronic polymicrobial infections.

In a first set of experiments, we aimed to understand the demographics of pathogen–host interactions in single species (mono) infections ($n = 30$–36 larvae per condition). For this purpose, we manipulated the injection dose and relative host age to understand how these factors affect each pathogen's virulence and mortality for the host. Second, we conducted mixed species infection experiments (double, triple and quadruple) to assess how polymicrobial infections affect virulence patterns and host survival ($n = 50$–60 larvae per condition). Third, we quantified pathogen growth within the host at two time points for all mono and pairwise infections to test whether pathogen load links to virulence ($n = 8$–12 larvae per condition). Fourth, we followed changes in pathogen frequencies in mixed infections to derive pathogen interaction patterns ($n = 8$–12 larvae per condition). While this approach does not reveal specific molecular mechanisms of pathogen interactions, it allows us to distinguish between negative, neutral and positive interactions between co-infecting pathogens and how such interactions link to virulence. One key insight from our experiments was that host mortality was always driven by the most virulent species, with the virulence of a pathogen correlating with its growth inside the host and its competitiveness towards the co-infecting species. Based on these insights, we predicted that the most virulent species should be targeted first in an infection to reduce host morbidity and mortality. In a follow-up experiment, we validated this prediction by specifically targeting the more virulent *P. aeruginosa* co-infecting the host together with the less virulent *B. cenocepacia* ($n = 48$–54 larvae per condition).

2. Material and methods

(a) Bacterial strains and host

We used the following four opportunistic human pathogens: *Pseudomonas aeruginosa* PAO1 [36], *Burkholderia cenocepacia* K56-2 [37], *Klebsiella michiganensis* and *Cronobacter sakazakii* (ATCC29004). We purchased the larvae of the greater wax moth *G. mellonella* in their last instar stage from a local vendor (Bait Express GmbH, Basel, Switzerland), who confirmed that their larvae had not been treated with any antibiotics. We can therefore rule out the possibility that pathogen interactions in our experiments are affected by residual antibiotic concentrations in the larvae. Upon arrival, we stored them at 4–8°C without food. We considered larval age as the number of days after arrival in our laboratory, since the exact age of larvae was unknown to us. Hence, we only investigated larval age as a relative measure. When examining relative larval age, we compared larvae that were ordered at the same time (i.e. same batch), but were infected at different time points. To put host age into a wider context, the *G. mellonella* life cycle comprises four developmental phases: egg (3–30 d), larva (6–7 weeks), pupa (6–55 d) and adult [38]. All our experiments involve larvae from the last (out of seven) larval stages [39]. At this stage, larvae have an active innate immunity [39]. They also naturally stop feeding when fully grown [39] so that the lack of food should not affect their general health condition. This notion is confirmed in our experiments with mock infections (0.8% NaCl), showing that relative age did not significantly affect larval survival (electronic supplementary material, figure S1).

(b) Culturing conditions of bacteria

Bacterial stocks were kept in 25% glycerol and stored at −80° C. For all experiments, we grew bacteria overnight until stationary phase in 5 ml lysogeny broth (LB) in 50 ml Falcon tubes at 37° C and at 170 rpm with aeration (Infors HT, Multitron Standard Shaker). For all species, we centrifuged 1 ml overnight-cell culture in a 1.5 ml Eppendorf tube at 7500 rcf for 5 min (Eppendorf, tabletop centrifuge MiniSpin plus with rotor F-45-12-11) and washed cultures three times with a 0.8% NaCl solution to remove all original media. Next, we measured the optical density at 600 nm (OD_{600}) of the washed cell culture (Amersham Biosciences, Ultrospec 2100 pro spectrophotometer), adjusted it to $OD_{600} = 1$ and diluted each species individually to obtain similar cell numbers per millilitre for all species.

While all our main experiments were carried out on the *G. mellonella* larvae, we conducted one additional *in vitro* experiment. Specifically, we grew all four pathogens as monocultures in a medium that mimics the haemolymph of Lepidoptera—the insect order to which *G. mellonella* belongs—called Grace's insect medium (GIM, electronic supplementary material, figure S2). The aim of this experiment was to show that our model host directly affects pathogen growth and is not just serving as a sack to conduct growth assays. Thus, we expected pathogen growth to be different inside the host compared to the *in vitro* GIM environment. We prepared bacterial overnight cultures as stated above to obtain washed and $OD_{600} = 1$ adjusted cell cultures. A 96-well cell culture plate (Eppendorf, non-treated, flat bottom) was then filled with 190 µl GIM (Gibco, GIM 1X, supplemented) and 10 µl cells to reach a starting $OD_{600} = 0.001$ per

well. To reduce evaporation the inter-well spaces and the outer moat space of the microplate were filled with sterile water (13 ml in total). We incubated the microplate at 37°C in a microplate reader (Tecan, Infinite MPlex, monochromator optics) and measured OD_{600} every 15 min for 24 h, shaking for 60 s before every read. The plate layout was randomized between experiments. All chemicals were purchased from Sigma Aldrich, Switzerland, unless indicated otherwise.

(c) Infection experiments

Prior to infections, we sorted larvae and evenly distributed them across treatments according to size. Their weight ranged from 278–731 mg with an average weight of 499 mg. We put larvae on ice in a Petri dish to immobilize them. Next, we surface-sterilized larvae with 70% ethanol and injected them between the posterior prolegs. We used a sterile hypodermic needle (Braun, 0.45 × 12 mm BI/LB, 26G), a sterile syringe (Braun, 0.01–1 ml Injekt-F Luer Solo) and a programmable syringe pump (New Era Pump Systems Inc, model NE-300) to standardize injection speed. With a flow rate of 2 ml h^{-1}, we injected either 10 µl control or bacterial solution (both in 0.8% NaCl) into larvae within 18 s. We had a second control treatment, where larvae were not injected. The injection dose ranged from 10^2 to 10^6 colony forming units (CFU) for mono infections and was kept at 10^5 CFU for experiments that included multispecies infections. In multispecies infections, we mixed equal amounts of each species. The order of treatments was randomized between experiments. For all experiments, we confirmed the injection dose in triplicate by CFU on 1.5% LB agar plates. We distributed injected larvae to individual wells of a 12-well plate for incubation at 37°C in the dark without food. We monitored survival of every larva at regular intervals (hourly during 12–24 h post infection (hpi) and every 2 h during 36–48 hpi). Larvae were considered dead when they did not move upon touch with a pipette tip.

We used gentamicin to selectively target P in co-infections with B. First, we determined the gentamicin concentration that killed P but had no effect on B *in vitro*, since B is inherently resistant to gentamicin (up to a certain concentration). We found that 8 µg ml^{-1} gentamicin fulfilled the condition. Thus, we injected 10 µl of a 400 µg ml^{-1} gentamicin solution into the larvae, which should result in an internal gentamicin concentration of 8 µg ml^{-1} based on the average larval weight (assuming 499 mg ~ 500 ml according to [40]). The gentamicin treatment was applied 2 h after the bacteria had been injected so that they had time to establish an infection in the host. To control for any impact caused by the second injection, half of the NaCl sterile control larvae also received the gentamicin treatment.

(d) Bacterial load in the haemolymph

We determined the bacterial load in all larvae that received mono-, mixed-, NaCl and no infection at two time points, at 6 and 12 hpi. Since larvae had to be sacrificed during this process, we had two independent batches of larvae that were used for the respective timepoints. First, we placed larvae individually in 2 ml Eppendorf tubes and submerged those in ice until larval movement halted. Then, we opened each larva with a surgical blade (Aesculap AG, Germany) behind the posterior prolegs, with the cut length spanning half of the body width. This procedure is similar to the one used by Harding *et al*. [41], McCloskey *et al*. [42] and Admella & Torrents [43]. We sterilized the blade with 70% ethanol between different larvae. Next, we drained 10–20 µl haemolymph into a fresh 1.5 ml Eppendorf tube by gently squeezing the larva. The collected haemolymph was mixed and stored on ice. To enumerate bacterial CFU, we serially diluted 10 µl of the collected haemolymph in 0.8% NaCl up to 10^{-6} and plated the appropriate dilutions on LB-agar plates (1.5% agar) in duplicates. The appropriate dilutions varied between 10^0 (undiluted) and 10^{-6} and depended on the bacterial species. We incubated the plates at 37° C overnight and then manually counted CFU. Because *B. cenocepacia* grew more slowly than the other species, plates were incubated for two days. Plates with *C. sakazakii* were kept at room temperature for an additional day following overnight incubation for colonies to develop their characteristic yellow colour. All four species could be distinguished from each other based on their different colony morphologies (see electronic supplementary material, figure S3). We considered plates with a minimum of 25 CFU up to a number of CFU for which we could still distinguish single colonies with confidence. Plates with fewer than 25 CFU were only considered if none of the plated dilutions from the same individual adhered to this threshold. For mixes where one species occurred at very low frequency (mostly mixes with P), we plated the undiluted haemolymph to see whether the rare species was present at all. While both C and K were visible even in a lawn of P, this was not true for B. For this species combination, we cannot conclude that B was completely absent in certain larvae but rather that P was highly dominant. We calculated the CFU/larva by multiplying the volume of plated haemolymph with the average larval weight since larval weight is almost identical to larval liquid volume according to Andrea *et al*. [40].

In approximately 20% of the extracted larval haemolymph, we detected different bacteria from our four focal species. We determined the identity of ten representative isolates by 16S rRNA sequencing (colony PCR using standard primers 1492r and 27f). We identified *Enterococcus casseliflavus* and *E. gallinarum*, two common insect gut bacteria [44,45], as the closest relatives of our isolates with sequence identities of 89–99%. These results suggest that we had drained certain larvae too extensively, such that bacteria had been collected not only from the haemolymph but also from the gut. For this reason, we excluded these larvae from all further analyses.

(e) Statistical analyses

All statistical analyses were performed with R (v. 4.1.1) and the interface RStudio (v. 2021.09.0) [46]. For the dose–response curves in figure 1*a*, we measured mean survival time of the host as the area under the full survival curve using the function survmean from the survival package [47]. To build a log-logistic model we used the drm function from the drc package [48]. To compare host survival in mono versus mixed infections, we built a separate model for each panel shown in figure 2, comparing host survival of a particular pathogen combination. The statistical results were robust across three different methods comparing host survival: the non-parametric log-rank test, the semi-parametric Cox proportional hazards model and the parametric Weibull regression. See electronic supplementary material, table S1 for a model comparison. Non-parametric log-rank tests were also used to compare host survival between mono and mixed infections with or without gentamicin treatment (figure 5, electronic supplementary material, table S1).

To determine whether the pathogens significantly vary in their bacterial load in mono infections, we compared the CFU extracted from the haemolymph of host individuals at 6 hpi and 12 hpi. We chose a linear model using generalized least squares to account for differences in variance between the species, which was mainly caused by *K. michiganensis* at 12 hpi (see electronic supplementary material, table S2 for the full statistical analysis). Next, we performed a *post-hoc* analysis using the Tukey honest significant difference test with *p*-value adjustment to compare the bacterial load between species.

To compare bacterial load in the haemolymph in mono- versus mixed infections, we built a separate maximal linear model (electronic supplementary material, table S4) for each pathogen to test whether its growth was influenced by the presence of another species, the CFU of this other species, and time (at 6 hpi versus

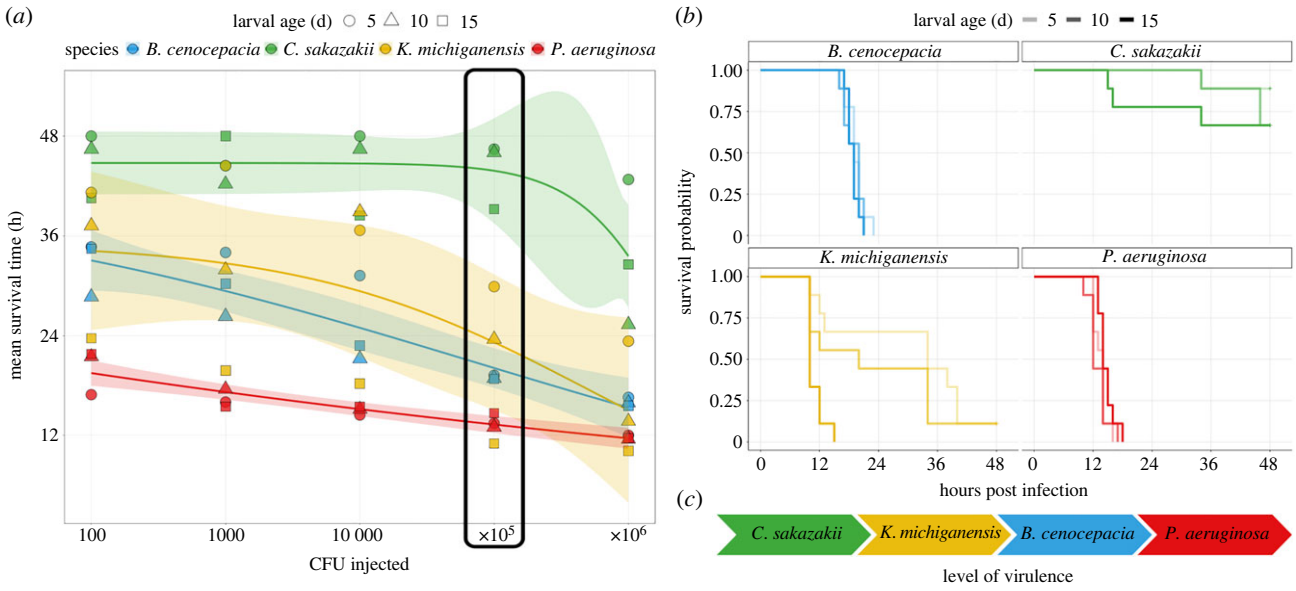

Figure 1. Survival rates of greater wax moth larvae (*G. mellonella*) are affected by the pathogen species with which they are infected, injection dose and relative larval age. (*a*) Mean survival time of *G. mellonella* larvae (measured as the area under the full survival curve) as a function of relative larval age (5, 10, 15 days), injection dose (colony forming units, CFU) and pathogen species (blue: *B. cenocepacia*, green: *C. sakazakii*, yellow: *K. michiganensis*, red: *P. aeruginosa*). The lines and the shaded areas (95% CI) depict the relationship between mean survival time (across the different relative larval ages and replicates) and infection dose for each species. The black box highlights the injection dose chosen for all subsequent experiments. (*b*) Kaplan Meier survival curves of *G. mellonella* larvae for an injection dose of 10^5—CFU for each of the four pathogen species. Relative larval age—5, 10 and 15 days after the arrival in our laboratory—is indicated by increasing line opaqueness. (*c*) The arrow chart shows the rank order of virulence among the four bacterial pathogens, from lowest to highest based on our experimental data. Data are from three independent experiments, each featuring 10–12 larvae per treatment, resulting in a total of 30–36 larvae per treatment.

12 hpi). Since the injection dose was always the same independent of how many species were injected, we compared for each species half the CFU found in mono infections to the total CFU (for the focal species) observed in pairwise infections. To obtain normally distributed residuals, we transformed all CFU values in our models. We used the function transformTukey from the rcompanion package to find the best transformation [49]. Testing for collinearity in the maximal model [50] showed that the presence of another species and its CFU were collinear with each other, as might be expected (all other combinations of terms showed no major collinearity). The structure of our data meant we could not account for the collinearity with a pairwise interaction. However, we always considered these two terms together (see below).

Non-significant interaction terms and main effects were removed from maximal models until a minimal model was obtained. Most of the minimal models included both a presence/absence effect of the co-infecting species and its CFU effect. Due to collinearity between these terms, and because these two explanatory variables often had opposing signs, we assessed the effect of these parameters together. To do this, we assessed the threshold CFU of the co-infecting pathogen at which its effect on the focal pathogen switches from being positive to being negative. This was done for each pathogen combination. We could then compare this CFU threshold to our experimental CFU values to check whether a co-infecting species stimulated or inhibited a focal species. To calculate the standard error for confidence intervals of this threshold and the *p*-value (one sample *t*-test versus zero) we used the first order Taylor expansion in the R package propagate [51].

3. Results

(a) Injection dose, relative host age and species identity determine virulence

To assess how the four different pathogens affect host survival, we exposed *G. mellonella* larvae (last instar larvae, relative age: 5, 10 or 15 days after arrival in our laboratory; see methods (§2a) for details on larval life cycle) to a range of pathogen injection doses (100 to 1 million CFU) for each of the four pathogens (B, C, K, P) and tracked their survival over 48 h (figure 1*a*,*b* and electronic supplementary material, figure S1).

We found that the risk of death differed between the four species (Cox proportional hazard: $\chi^2_3 = 308.6$, $p < 0.0001$) and was influenced by significant interactions between species and relative larval age ($\chi^2_3 = 67.28$, $p < 0.0001$) and between species and injection dose ($\chi^2_3 = 10.96$, $p = 0.0119$). When examining these interactions more closely, we observed that the risk of death grew significantly with increasing relative larval age for C ($z = 2.69$, $p = 0.0071$) and K ($z = 6.43$, $p < 0.0001$), but only marginally for B ($z = 1.90$, $p = 0.0573$) and not at all for *P* ($z = -0.72$, $p = 0.471$). For the injection dose, we found that higher CFU significantly increased the risk of death in all four species, but the hazard increase was more pronounced for B and P than for K and C (see electronic supplementary material, table S3 for the full statistical analysis). The reason for the species-specific relationship between virulence and infection dose stems from the fact that the survival decreased in a log-linear fashion for B and P with higher pathogen doses, whereas C and K only became virulent above a certain threshold injection dose of about 10^4 CFU for K and 10^5 CFU for C.

Based on the insights from this experiment, we decided to use an injection dose of 10^5 CFU for all subsequent experiments. At this injection dose, all four pathogens are virulent with the following order of virulence: *P. aeruginosa* (P) > *B. cenocepacia* (B) > *K. michiganensis* (K) > *C. sakazakii* (C), and with significant relative host age effects for C and K (figure 1*c*).

(b) Host mortality in multispecies infections is determined by the most virulent species

Next, we compared host survival between mono and mixed infections. For this, we injected pairwise combinations of

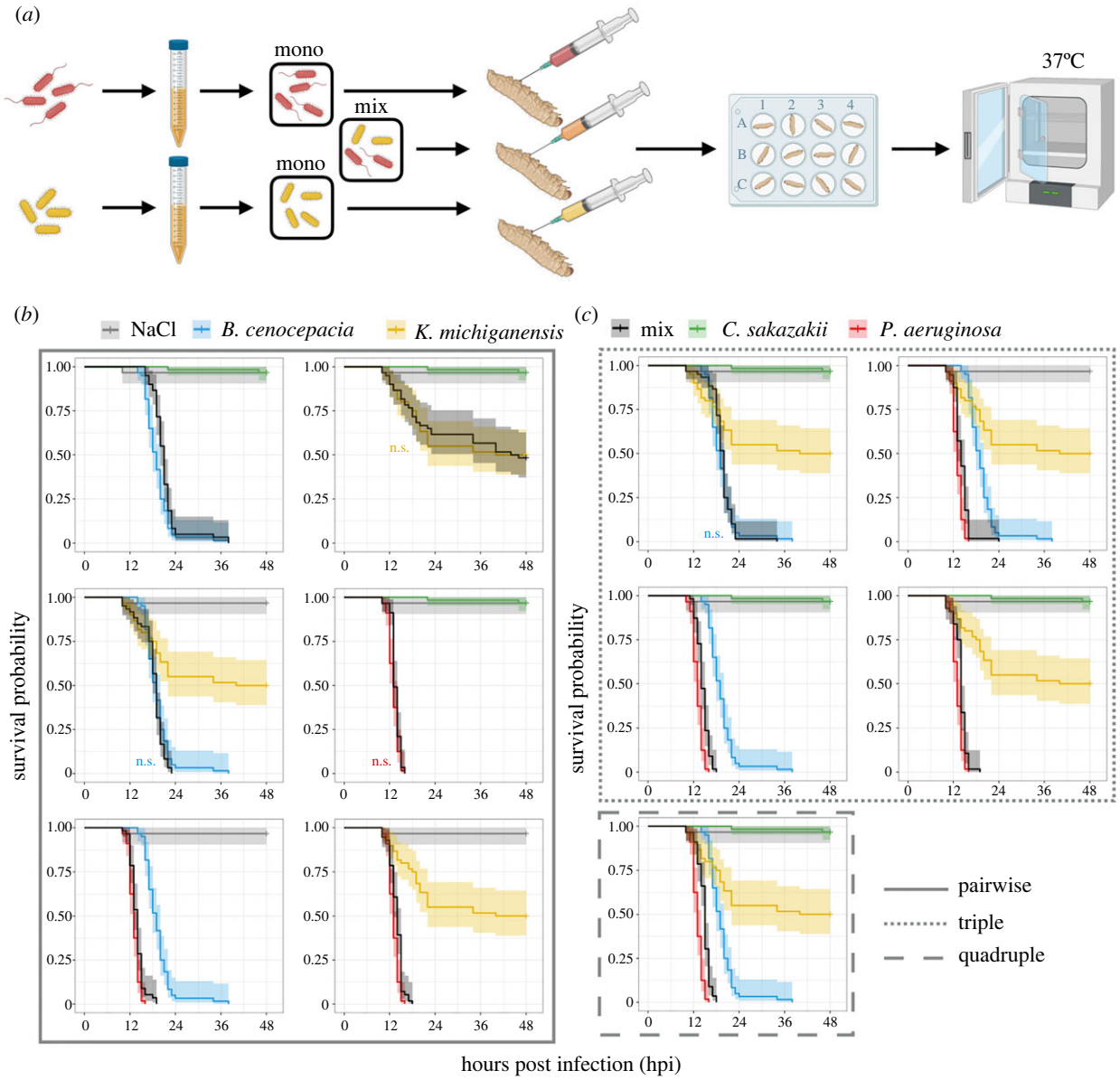

Figure 2. Host survival dynamics of *G. mellonella* larvae of pairwise, triple and quadruple bacterial infections follow the pattern of the mono infection (coloured curves) of the most virulent pathogen in a mix (black curves depict the mix of all pathogens within the respective panel). (*a*) Schematic overview of the experimental setup, with the example of the mono and pairwise infections of *P. aeruginosa* (red) and *K. michiganensis* (yellow). A total of 10^5 CFU were injected into *G. mellonella* larvae with equal amounts of each species in a mix. Kaplan Meier survival curves of (*b*) mono versus pairwise and (*c*) triple and quadruple infections, with the shaded areas indicating the 95% CI. The denotation ns (non-significance) marks cases for which survival does not significantly differ between one of the mono infections compared to the mixed infection in the same panel. Data are from five independent experiments, each with 10–12 larvae per treatment, resulting in a total of 50–60 larvae per treatment.

our four bacterial species into larvae of *G. mellonella* and observed their survival over 48 h (figure 2*a*). The injection dose was always 10^5 CFU in total, with equal amounts of each co-injected species. We found that any pairwise infection followed the dynamics of its most virulent species (figure 2*b*). A statistical examination confirmed that larval survival was not different between the mixed infection and the mono infection of the more virulent species in three out of six cases (log-rank test B + K versus B: $p = 0.2459$; C + K versus K: $p = 0.9770$; C + P versus P: $p = 0.0548$). In the remaining three cases, survival in the mixed infection was significantly lower than in the mono infection of the more virulent species (B + C versus B: $p = 0.0033$; B + P versus P: $p = 0.0230$; K + P versus P: $p = 0.0041$), but the actual biological differences observed are extremely small (figure 2*b*).

We then tested whether the same patterns arise in the four triple and the quadruple infections. As above, we kept the total number of CFU constant at 10^5 CFU and mixed equal amounts of each pathogen. As for the paired infections, we found that the survival trajectory of larvae infected with three and four pathogens followed the trajectories of the mono infection of the most virulent species in the mix (figure 2*c*). For example, in the triple infection with B, C and K, larval survival followed the one of the B mono-infection, which is the most virulent of the three species. In the remaining four mixes, the most virulent species was P and in all these cases larval survival followed the one of P mono infections. Statistical analyses revealed subtle but significant differences: mixed infections with P were always slightly less virulent than the mono infections with P (see electronic supplementary material, table S1 for the full statistical analysis). We can explain this pattern by a density effect: fewer P cells were injected in higher-order infections, and thus bacteria needed more time to replicate and reach

sufficiently high numbers to kill the larval host (electronic supplementary material, figure S4).

(c) The most virulent species is also more abundant both in mono and mixed infections

We then asked what the underlying reason could be for our observation that the most virulent species drives host survival dynamics. One explanation would be that the more virulent species grows better in the host, making it more abundant and thereby exerting a stronger effect on the host. We tested this hypothesis in mono infections first and found that bacterial load (CFU per larva) of the four pathogens followed the exact order of their virulence at 12 h post infection (hpi, see electronic supplementary material, figure S5 and electronic supplementary material, table S2 for the full statistical analysis). At the earlier timepoint (6 hpi), the same pattern holds for B, C and P, whereas K had much higher CFU inside the host than expected from its virulence. The data imply that K initially grows well in larvae, while it is compromised later during the infection. Overall, the mono infection data suggest that pathogen load in a host positively links to its level of virulence (i.e. negatively with host survival).

Next, we explored whether the same is true for mixed infections, i.e. whether the dominant effect of the more virulent species might be caused by its higher abundance in a co-infection. Indeed, in all cases the more virulent species was also the more abundant species at 12 hpi (figure 3). For example, as the most virulent of our pathogens, P dominated in terms of abundance in all larvae in any of its mixes at 12 hpi. However, we also found evidence for more complex dynamics, where relative species abundance changed over time. Especially in the infection pairs K + P and K + B, we observed that K dominated at 6 hpi despite being the less virulent species, a pattern that disappeared at 12 hpi. It is important to note that in five out of six pairings both pathogen species coexisted in the host during the course of the infection in a large proportion of larvae.

(d) Negative interactions dominate in pairwise infections

We used the CFU data from mixed infections to test whether the growth of any of the four species was influenced by the presence of a co-infecting species across two time points (at 6 and 12 hpi). We found that the co-infecting species had either no effect or a negative effect on a focal species in a pathogen-pair specific way (figure 4; see electronic supplementary material, table S4 for the full statistical analysis). The negative effect was either independent of the co-infecting species' prevalence (presence/absence effect) or stronger with increasing CFU of the co-infecting species (CFU effect).

(B): The growth of this pathogen increased from 6 hpi to 12 hpi ($t_{77} = 2.66$, $p = 0.0095$) and was not affected by C ($t_{77} = -0.10$, $p = 0.9171$). By contrast, B growth was compromised by increasing numbers of K at the earlier timepoint and P at both timepoints (CFU effect of second species, for K: $t_{77} = -4.73$, $p < 0.0001$; for P: $t_{77} = -4.17$, $p < 0.0001$). The presence of P at 12 hpi resulted in a CFU drop of B even below the inoculum size in many larvae.

(C): In mono infections, this pathogen's CFU dropped below the inoculum size at both timepoints, suggesting that it cannot replicate within the host within the first 12 h. Given that C can kill larvae (at high infection doses and in larvae with increased relative age; figure 1 and electronic supplementary material, figure S1), we assume that C starts replicating at later time points in mono infections. We found that the presence of B did not affect C at any given time, while both K and P significantly compromised C abundance (presence/absence effect, for K: $t_{66} = -3.29$, $p = 0.0016$; for P: $t_{66} = -2.20$, $p = 0.0314$).

(K): In line with the host survival data (figure 1*a*,*b*), we found more CFU of this pathogen when the larval host was relatively older ($t_{71} = 4.27$, $p < 0.0001$). The growth of K significantly decreased with higher CFU of the co-infecting B at both timepoints (CFU effect of B: $t_{71} = -2.48$, $p = 0.0156$). Interestingly, our model predicts that K reaches higher CFU if C is present at sufficiently high numbers (CFU effect of C: $t_{71} = 2.90$, $p = 0.0050$), but because C never reached high CFU itself, the overall effect of C on K was negative in our experiments (presence/absence effect of C: $t_{71} = -2.92$, $p < 0.0047$).

(P): The CFU of P significantly increased from 6 to 12 hpi ($t_{73} = 9.89$, $p < 0.0001$). P growth was only affected by K, which had a strong negative impact at 6 hpi (CFU effect of K: $t_{73} = -4.40$, $p < 0.0001$).

While the number of interactions decreased over time (58% at 6 hpi; 42% at 12 hpi), all significant interactions were negative at both timepoints. Our four bacterial species spanned from being inhibited by one (P) or two other species (B, C, K) and inhibiting one (B, C), two (P) or three (K) other species (figure 4*b*). At 12 hpi, the competitive strength of the four pathogens followed their order of virulence and growth, whereby P suppresses B and C; B suppresses K; and K and C mutually repress each other, with the former being slightly stronger.

(e) Targeting the more virulent species in mixed infections increases host survival

The main conclusion of the above results is that there are positive associations between a pathogen's growth inside the host, its competitiveness towards other pathogens, and its virulence. Consequently, we predicted that treating the most virulent species in a multispecies bacterial infection would be an effective strategy to increase host survival. To test this prediction, we co-infected *G. mellonella* larvae with B + P and compared host survival of the mixed infection to the mono infections of B and P, with all conditions receiving either no treatment or a single dose of gentamicin after two hours. Given that B is inherently resistant to gentamicin, we predicted that the more virulent pathogen P should be selectively killed, and the survival dynamics of the mixed infection should follow the one of the B mono infection.

In the absence of gentamicin, we recovered our previous findings (figure 2*b*) that mixed B + P infections followed the virulence trajectory of P mono infections (figure 5; see electronic supplementary material, table S5 for the full statistical analysis). In stark contrast and in support of our prediction, we observed that host survival in B + P mixed infections more closely followed the trajectory of the B mono infection under gentamicin treatment (figure 5). This finding suggests that P was selectively removed by gentamicin, which is supported by our mono infection data showing that larval

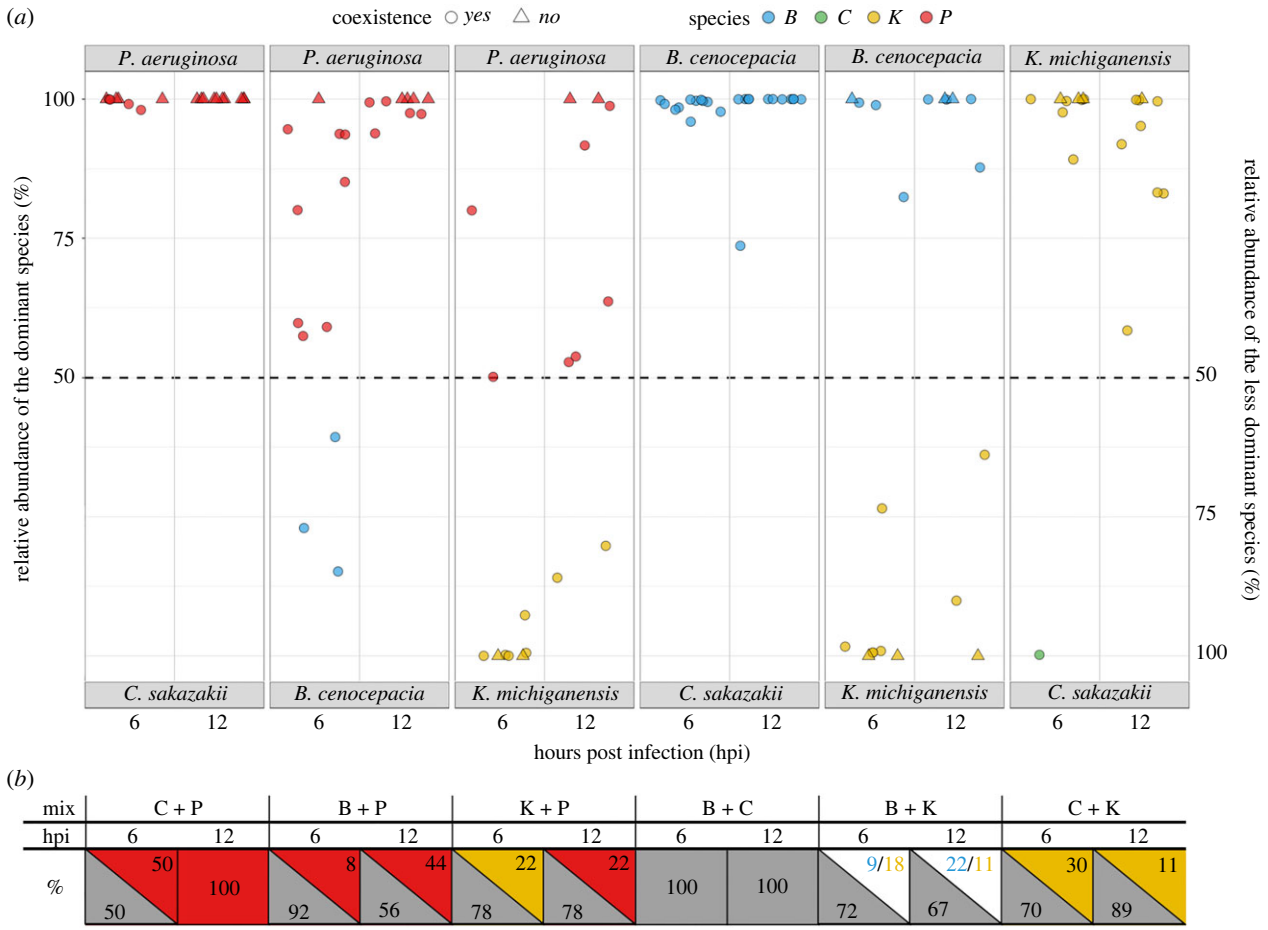

Figure 3. The more virulent pathogen is more abundant in pairwise infections and coexistence can occur in five out of six pairings throughout the infection. (*a*) Relative abundance in pairwise infections of *G. mellonella* larvae at 6 and 12 h post infection (hpi). The panels follow the order of the more virulent species in the mix, from left to right, with the more dominant species being labelled on top of each panel. The left and right *y*-axes show the relative abundance of the more dominant and less dominant species, respectively. Each datapoint represents one larva and is coloured according to the more abundant pathogen species found in the larva. Circular datapoints represent pairwise infections in which both pathogens were found at 6 hpi or 12 hpi and triangles indicate datapoints for which only one of the injected species remained in the host (or the rarer species was below detection limit). (*b*) Rectangles and triangles show the percentage of larvae in which either coexistence (grey) of pathogens occurred or only a single species (colour) was left. Data are shown for all pairwise infections both at 6 hpi and 12 hpi. Data are from 4–5 individual experiments with 2–3 larvae per treatment, resulting in a total of 8–12 larvae per treatment.

survival is very high for the P infection treated with gentamicin. Overall, B + P infections treated with gentamicin were significantly less virulent than B + P infections not receiving gentamicin treatment (log-rank test: B + P + gentamicin versus B + P: $p < 0.0001$). These results support the view that treating the most virulent species first in a polymicrobial infection is a promising strategy to reduce host mortality.

4. Discussion

There is increasing evidence that polymicrobial infections are common [1–4] and that ecological and evolutionary interactions between co-infecting pathogens can affect host morbidity [7–9]. In our study, we examined whether there are generalizable patterns that characterize interaction dynamics between pathogens and a common host in multi-species infections. For our experiments, we used the larvae of *G. mellonella* as the host and infected it with four opportunistic human bacterial pathogens alone and in all possible combinations of mixed infections. We tested the rank order of virulence for the four pathogens and found that it was identical to the rank order of growth in the host. In addition, the more virulent species in mono infections were also better at outcompeting other species in mixed infections. A consequence of this was that the most virulent species determined host survival dynamics in mixed infections regardless of the number and type of pathogens mixed. Our findings, which held for all pathogen combinations tested, reveal an infection dynamic that seems intuitive but is not covered by any of the current models for pathogen virulence in mixed infections.

While we found that the virulence of a specific pathogen is positively linked to its growth and competitiveness in the host, our co-occurrence analysis could give us an idea of the relative importance of pathogen growth versus competitiveness and how it varies across pathogen species combinations (figure 4). In the pathogen interaction network (figure 4*b*), the absence of an interaction suggests that differences in growth dominate a co-infection, meaning that the faster-growing species simply outperformed the slower-growing one. This was the case for five (6 hpi) and seven (12 hpi) out of the total twelve interactions. Conversely, the remaining seven (6 hpi) and five (12 hpi) interactions that were negative would imply that competitiveness played a more prominent role. At least two types of competition could be involved. First, the faster-growing species limits resource availability for the slow-growing species, reducing its growth and survival due to starvation. Second, the more

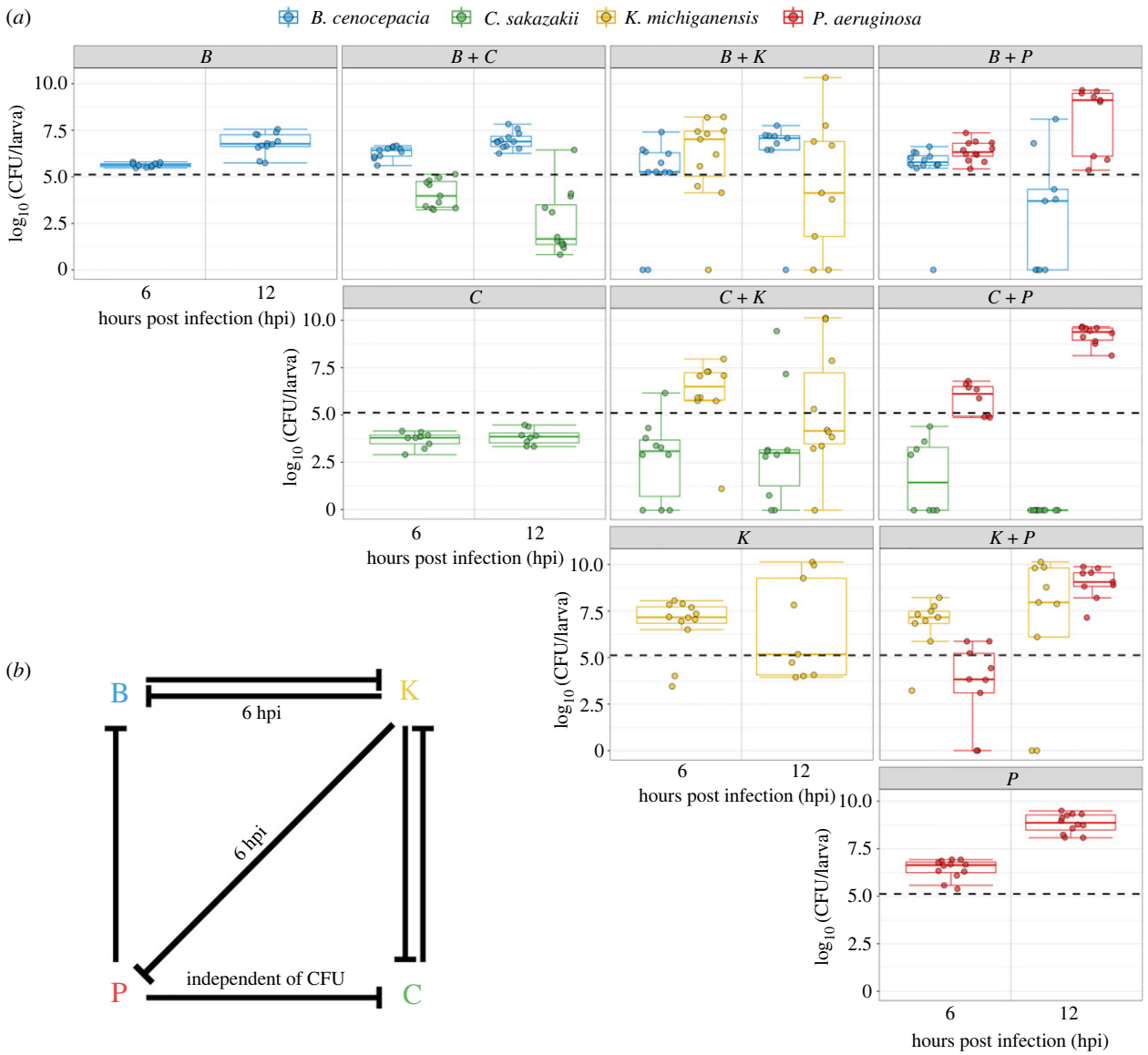

Figure 4. Bacterial load in *G. mellonella* larvae infected with a single pathogen or pairs of pathogens 6 and 12 h post infection (hpi). (*a*) Boxplots depict the number of CFU per larva for the mono infections of B, C, K and P, and all pairwise infections for the two time points measured. Dots represent data from individual larvae. The dashed black line shows the injection dose of 50 000 CFU per species in mixed infections. The dose for mono infections was 100 000 CFU. To be able to directly compare the CFU between mono and mixed infections, we halved the actual CFU counts obtained from the mono infections. Boxplots show the median (line within the box) with the first and third quartiles. The whiskers cover 1.5× of the interquartile range or extend from the lowest to the highest value if all values fall within the 1.5× interquartile range. Data are from 4–5 individual experiments, each featuring 2–3 larvae per treatment, resulting in a total of 8–12 larvae per treatment. (*b*) Interaction network of our bacterial consortium based on the statistical analysis of the data for both timepoints unless indicated otherwise. Significant negative impact of one species on another is depicted by a stop arrow. The label 'independent of CFU' indicates that this effect was not determined by the abundance of the co-infecting pathogen.

competitive species secretes a toxin or deploys contact-dependent mechanisms to target and kill the less competitive species in interference competition. While our results do not allow differentiation between resource and interference competition [52], it is likely that both mechanisms matter. For example, in our mixed infections with K + B, and K + P, we observed that K inhibits its competitors early on during the infections (6 hpi) but is outcompeted at a later stage (12 hpi). One option is that the inhibitory effects early during the infection could be explained by K secreting a toxin, while the dominance of B and P later in the infection could be due to resource competition advantages. Alternatively, it could be that K grows quickly but inefficiently while its competitors (B and P) grow more slowly but efficiently and thus outpace K over time.

It is also important to note that all pathogen interactions were either negative or neutral, but never positive. This finding supports the view that competition is much more prevalent between bacterial species than positive interactions, where one species unilaterally or mutually benefits another species [53,54]. The prevalence of competitive interactions is perhaps expected given that the pathogens interacted in a closed environment (i.e. the larva), where both resource availability and host longevity are limited [55]. It is worth noting that C might take on a special role among our panel of pathogens, because it did not replicate inside the host within the timeframe of the CFU enumeration experiments. C could therefore be a bystander in mixed infections with more virulent species. For this reason, the biological relevance of the negative interaction with K revealed by our model needs to be interpreted with caution.

Competition between pathogens is also a major component of mathematical models predicting virulence levels

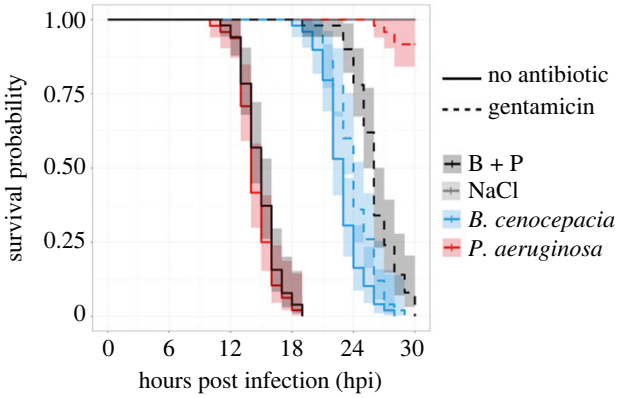

Figure 5. Treating the more virulent pathogen reduces host mortality in mixed infections to the level of the less virulent pathogen. Kaplan Meier survival curves of *G. mellonella* larvae injected with either NaCl (control, grey), B (less virulent pathogen, blue), P (more virulent pathogen, red), or B + P mixes (black). Larvae received either a gentamicin treatment (dashed lines) two hours after the bacterial/NaCl injection or no antibiotic treatment (solid lines). Survival curves are based on a total of 48–54 larvae per treatment from three independent experiments.

[56]. A traditional set of models assumes that genetically diverse pathogens engage in increased levels of resource competition in mixed infections, which is predicted to exacerbate virulence [55]. Other models examined the effect of infighting between pathogens through toxin secretion [57] or competition for publicly shared virulence factors [58]. These models predict that increased competition between pathogens should decrease virulence in mixed infections. Empirical support for these models varies, indicating that both types of predictions can apply [59–62]. A key insight from these studies is that the biological details of pathogen interactions matter. While our study was not designed to test specific model predictions, our results put forth an additional virulence scenario, namely that pathogen interactions in mixed infections neither increase nor decrease virulence, but the virulence trajectory simply follows that of the more harmful species. Such a virulence scenario can arise when pathogen traits that are relevant for infections—virulence, growth, competitiveness—are positively related to one another. A first example of this scenario was reported by Massey *et al*. [61] and here we reveal its generality. This virulence model could be particularly relevant for infections with opportunistic pathogens that co-incidentally end up in the same host with no prior interaction and coevolution history [3]. Moreover, the scenario could often apply in cases where certain pathogens are highly virulent, like B and P in our study that killed 100% of the larvae irrespective of the inoculum size (figure 1 and electronic supplementary material, figure S1).

Our data further indicate that host factors also influence pathogen virulence patterns. For example, we found that larval susceptibility to disease increased with relative age when infected with B, C, and K. Given that *G. mellonella* has an innate immune system similar to the one of vertebrates, our results indicate that the immune response works well against less virulent pathogens (like C and K) but deteriorates with relative age (i.e. number of days after the arrival of the larvae in our laboratory). Another host effect we observed is that *G. mellonella* managed to control infections of C and K at low injection doses, again highlighting the potency of the insect's immune system. A further indication that pathogen performance is modulated by the host stems from an additional experiment, which we conducted with a medium that mimics the haemolymph of the insect order Lepidoptera (electronic supplementary material, figure S2). Although this medium nutritionally matches insect conditions, we found the rank order of pathogen species growth to be markedly different compared to growth in live hosts (insect condition *in vitro*: C > P > K > B versus *in vivo*: P > B > K > C). Clearly, host effects are important and likely feed back on pathogen–pathogen interactions, which is why they should be considered in future work on polymicrobial infections. Particularly, the rank order and dynamics between species might depend on the host, and it thus remains to be tested whether our findings hold true for other hosts like humans.

In conclusion, we can draw two generalities from our four-bacteria-infection system. First, no matter what pathogen combination we used, the most virulent pathogen dictated host survival. This led us to predict that targeting the most virulent pathogen seems a promising strategy to reduce host morbidity/mortality in polymicrobial infections. We found support for this prediction in a proof-of-principle experiment, where we selectively targeted the more virulent species in a mixed infection with antibiotics. Second, more virulent pathogens grow better in the host and are better in competition with less virulent pathogens. These observations suggest that the same traits (or co-regulated traits) responsible for attacking the host (e.g. virulence factors) could promote pathogen growth and help in competition with other pathogens. Identifying these traits could give rise to promising strategies to control polymicrobial infections.

Ethics. This work did not require ethical approval from a human subject or animal welfare committee.

Data accessibility. The data are provided online at Data Dryad: https://doi.org/10.5061/dryad.z08kprrjj [63].

Additional information is provided in the electronic supplementary material [64].

Authors' contributions. D.A.S.: conceptualization, data curation, formal analysis, investigation, methodology, validation, visualization, writing—original draft, writing—review and editing; R.C.A.: formal analysis, writing—review and editing; R.K.: conceptualization, funding acquisition, project administration, resources, supervision, writing—original draft, writing—review and editing.

All authors gave final approval for publication and agreed to be held accountable for the work performed therein.

Conflict of interest declaration. We declare we have no competing interests.

Funding. This project has received funding from the Swiss National Science Foundation (grant no. 31003A_182499 to R.K.) and from the Novartis Foundation for Medical-Biological Research (to R.K.).

Acknowledgements. We thank Kayla King, Anna-Liisa Laine, Alex Hall and Roland Regoes for their scientific inputs. We also thank Nadine Koch for showing us how to conduct injections with the larvae of *G. mellonella*.

References

1. Peters BM, Jabra-Rizk MA, Costerton JW, Shirtliff ME. 2012 Polymicrobial interactions: impact on pathogenesis and human disease. *Clin. Microbiol. Rev.* **25**, 193–213. (doi:10.1128/CMR.00013-11)

2. Brogden KA, Guthmiller JM, Taylor CE. 2005 Human polymicrobial infections. *Lancet*

365, 253–255. (https://www.ncbi.nlm.nih.gov/pmc/articles/PMC7119324/)

3. Short FL, Murdoch SL, Ryan RP. 2014 Polybacterial human disease: the ills of social networking. *Trends Microbiol.* **22**, 508–516. (doi:10.1016/j.tim.2014.05.007)
4. Folkesson A, Jelsbak L, Yang L, Johansen HK, Ciofu O, Hoiby N, Molin S. 2012 Adaptation of *Pseudomonas aeruginosa* to the cystic fibrosis airway: an evolutionary perspective. *Nat. Rev. Microbiol.* **10**, 841–851. (doi:10.1038/nrmicro2907)
5. Citron DM, Goldstein EJC, Merriam CV, Lipsky BA, Abramson MA. 2007 Bacteriology of moderate-to-severe diabetic foot infections and in vitro activity of antimicrobial agents. *J. Clin. Microbiol.* **45**, 2819–2828. (doi:10.1128/JCM.00551-07)
6. Cuthbertson L *et al*. 2020 Lung function and microbiota diversity in cystic fibrosis. *Microbiome* **8**, 45. (doi:10.1186/s40168-020-00810-3)
7. Rezzoagli C, Granato ET, Kümmerli R. 2019 Harnessing bacterial interactions to manage infections: a review on the opportunistic pathogen *Pseudomonas aeruginosa* as a case example. *J. Med. Microbiol.* **68**, 1–15. (doi:10.1099/jmm.0.000873)
8. Stacy A, Everett J, Jorth P, Trivedi U, Rumbaugh KP, Whiteley M. 2014 Bacterial fight-and-flight responses enhance virulence in a polymicrobial infection. *Proc. Natl Acad. Sci. USA* **111**, 7819–7824. (doi:10.1073/pnas.1400586111)
9. Korgaonkar A, Trivedi U, Rumbaugh KP, Whiteley M. 2013 Community surveillance enhances *Pseudomonas aeruginosa* virulence during polymicrobial infection. *Proc. Natl Acad. Sci. USA* **110**, 1059–1064. (doi:10.1073/pnas.1214550110)
10. Frank SA. 1992 Models of plant–pathogen coevolution. *Trends Genet.* **8**, 213–219. (doi:10.1016/0168-9525(92)90236-w)
11. Frank SA. 1993 Coevolutionary genetics of plants and pathogens. *Evol. Ecol.* **7**, 45–75. (doi:10.1007/BF01237734)
12. Van Baalen M. 1998 Coevolution of recovery ability and virulence. *Proc. R. Soc. Lond. B* **265**, 317–325. (doi:10.1098/rspb.1998.0298)
13. Buckling A, Rainey PB. 2002 Antagonistic coevolution between a bacterium and a bacteriophage. *Proc. R. Soc. Lond. B* **269**, 931–936. (doi:10.1098/rspb.2001.1945)
14. Nourmohammad A, Otwinowski J, Plotkin JB. 2016 Host-pathogen coevolution and the emergence of broadly neutralizing antibodies in chronic infections. *PLoS Genet.* **12**, 1–23. (doi:10.1371/journal.pgen.1006171)
15. Papkou A *et al*. 2019 The genomic basis of red queen dynamics during rapid reciprocal host–pathogen coevolution. *Proc. Natl Acad. Sci. USA* **116**, 923–928. (doi:10.1073/pnas.1810402116)
16. Limoli DH, Hoffman LR. 2019 Help, hinder, hide and harm: what can we learn from the interactions between *Pseudomonas aeruginosa* and *Staphylococcus aureus* during respiratory infections? *BMJ* **74**, 684–692.
17. Orazi G, Ruoff KL, O'Toole GA. 2019 *Pseudomonas aeruginosa* increases the sensitivity of biofilm-grown *Staphylococcus aureus* to membrane-targeting antiseptics and antibiotics. *mBio* **10**, 1–15. (doi:10.1128/mBio.01501-19)
18. Tognon M, Köhler T, Luscher A, Van Delden C. 2019 Transcriptional profiling of *Pseudomonas aeruginosa* and *Staphylococcus aureus* during in vitro co-culture. *BMC Genom.* **20**, 1–15. (doi:10.1186/s12864-018-5398-y)
19. Niggli S, Kümmerli R. 2020 Strain background, species frequency, and environmental conditions are important in determining *Pseudomonas aeruginosa* and *Staphylococcus aureus* population dynamics and species coexistence. *Appl. Environ. Microbiol.* **86**, 1–14. (doi:10.1128/AEM.00962-20)
20. Sheehan G, Garvey A, Croke M, Kavanagh K. 2018 Innate humoral immune defences in mammals and insects: the same, with differences? *Virulence* **9**, 1625–1639. (doi:10.1080/21505594.2018.1526531)
21. Tsai CJY, Loh JMS, Proft T. 2016 *Galleria mellonella* infection models for the study of bacterial diseases and for antimicrobial drug testing. *Virulence* **7**, 214–229. (doi:10.1080/21505594.2015.1135289)
22. Ramarao N, Nielsen-Leroux C, Lereclus D. 2012 The insect *Galleria mellonella* as a powerful infection model to investigate bacterial pathogenesis. *J. Vis. Exp.* **70**, 1–7. (doi:10.3791/4392)
23. Junqueira JC. 2012 *Galleria mellonella* as a model host for human pathogens: recent studies and new perspectives. *Virulence* **3**, 474–476. (doi:10.4161/viru.22493)
24. Revuz J *et al*. 1987 Toxic epidermal necrolysis. *Arch. Dermatol.* **123**, 1160–1165. (doi:10.1001/archderm.1987.01660330071012)
25. Gaynes R, Edwards JR. 2005 Overview of nosocomial infections caused by gram-negative bacilli. *Clin. Infect. Dis.* **41**, 848–854. (doi:10.1086/432803)
26. Vandamme P *et al*. 1997 Occurrence of Multiple Genomovars of *Burkholderia cepacia* in cystic fibrosis patients and proposal of *Burkholderia multivorans* sp. nov. *Int. J. Syst. Bacteriol.* **47**, 1188–1200. (doi:10.1099/00207713-47-4-1188)
27. Yang J, Long H, Hu Y, Feng Y, McNally A, Zong Z. 2022 *Klebsiella oxytoca* complex: update on taxonomy, antimicrobial resistance, and virulence. *Clin. Microbiol. Rev.* **35**, 1–39. (doi:10.1128/CMR.00006-21)
28. Podschun R, Ullmann U. 1998 *Klebsiella* spp. as nosocomial pathogens: epidemiology, taxonomy, typing methods, and pathogenicity factors. *Clin. Microbiol. Rev.* **11**, 589–603. (doi:10.1128/CMR.11.4.589)
29. Högenauer C *et al*. 2006 *Klebsiella oxytoca* as a causative organism of antibiotic-associated hemorrhagic colitis. *N Engl. J. Med.* **355**, 2418–2426. (doi:10.1056/NEJMoa054765)
30. Neog N, Phukan U, Puzari M, Sharma M, Chetia P. 2021 *Klebsiella oxytoca* and emerging nosocomial infections. *Curr. Microbiol.* **78**, 1115–1123. (doi:10.1007/s00284-021-02402-2)
31. Iversen C *et al*. 2007 The taxonomy of *Enterobacter sakazakii*: Proposal of a new genus *Cronobacter* gen. nov. and descriptions of *Cronobacter sakazakii* comb. nov. *Cronobacter sakazakii* subsp. *sakazakii*, comb. nov., *Cronobacter sakazakii* subsp. *malonaticus* subsp. nov., *Cronobacter turicensis* sp. nov., *Cronobacter muytjensii* sp. nov., *Cronobacter dublinensis* sp. nov. and *Cronobacter* genomospecies 1. *BMC Evol. Biol.* **7**, 1–11. (doi:10.1186/1471-2148-7-64)
32. Govan JRW, Deretic V. 1996 Microbial pathogenesis in cystic fibrosis: mucoid *Pseudomonas aeruginosa* and *Burkholderia cepacia*. *Microbiol Rev.* **60**, 539–574. (doi:10.1128/mr.60.3.539-574.1996)
33. Eberl L, Tümmler B. 2004 *Pseudomonas aeruginosa* and *Burkholderia cepacia* in cystic fibrosis: genome evolution, interactions and adaptation. *Int. J. Med. Microbiol.* **294**, 123–131. (doi:10.1016/j.ijmm.2004.06.022)
34. Abbas HA, El-Masry EM, Shaker GH. 2013 Bacterial etiology and antimicrobial resistance of burn wound infections in a burn unit in Hehia General Hospital in Egypt. *Int. J. Biol. Pharm. Res.* **4**, 1251–1255.
35. Forson OA, Ayanka E, Olu-Taiwo M, Pappoe-Ashong PJ, Ayeh-Kumi PJ. 2017 Bacterial infections in burn wound patients at a tertiary teaching hospital in Accra, Ghana. *Ann. Burns Fire Disasters* **30**, 116–120.
36. Stover CK *et al*. 2000 Complete genome sequence of *Pseudomonas aeruginosa* PAO1, an opportunistic pathogen. *Nature* **406**, 959–964. (doi:10.1038/35023079)
37. Mahenthiralingam E, Coenye T, Chung JW, Speert DP, Govan JRW, Taylor P, Vandamme P. 2000 Diagnostically and experimentally useful panel of strains from the *Burkholderia cepacia* complex. *J. Clin. Microbiol.* **38**, 910–913. (doi:10.1128/JCM.38.2.910-913.2000)
38. Ellis JD, Graham JR, Mortensen A. 2013 Standard methods for wax moth research. *J. Apic Res.* **52**, 1–17. (doi:10.3896/IBRA.1.52.1.10)
39. Wojda I, Staniec B, Sułek M, Kordaczuk J. 2020 The greater wax moth *Galleria mellonella*: biology and use in immune studies. *Pathog. Dis.* **78**, 1–15. (doi:10.1093/femspd/ftaa057)
40. Andrea A, Krogfelt KA, Jenssen H. 2019 Methods and challenges of using the greater wax moth (*Galleria mellonella*) as a model organism in antimicrobial compound discovery. *Microorganisms* **7**, 1–9. (doi:10.3390/microorganisms7030085)
41. Harding CR, Schroeder GN, Collins JW, Frankel G. 2013 Use of *Galleria mellonella* as a model organism to study *Legionella pneumophila* infection. *J. Vis. Exp.* **81**, 1–10. (doi:10.3791/50964)
42. McCloskey AP *et al*. 2019 Investigating the in vivo antimicrobial activity of a self-assembling peptide hydrogel using a *Galleria mellonella* infection model. *ACS Omega* **4**, 2584–2589. (doi:10.1021/acsomega.8b03578)
43. Admella J, Torrents E. 2022 A Straightforward method for the isolation and cultivation of *Galleria mellonella* hemocytes. *Int. J. Mol. Sci.* **23**, 1–14. (doi:10.3390/ijms232113483)
44. Peng BY *et al*. 2019 Biodegradation of polystyrene by dark (*Tenebrio obscurus*) and yellow (*Tenebrio molitor*) mealworms (Coleoptera: Tenebrionidae). *Environ. Sci. Technol.* **53**, 5256–5265. (doi:10.1021/acs.est.8b06963)

45. Allonsius CN, Van Beeck W, De Boeck I, Wittouck S, Lebeer S. 2019 The microbiome of the invertebrate model host *Galleria mellonella* is dominated by *Enterococcus*. *Anim Microbiome.* **1**, 1–7. (doi:10.1186/s42523-019-0010-6)
46. R Core Team. 2021 *R: A language and environment for statistical computing*. Vienna, Austria: R Foundation for Statistical Computing.
47. Therneau TM, Grambsch PM. 2000 *Modeling survival data: extending the Cox model*. New York, NY: Springer.
48. Ritz C, Baty F, Streibig JC, Gerhard D. 2015 Dose-Response Analysis Using R. *PLoS ONE* **10**, e0146021. (doi:10.1371/journal.pone.0146021)
49. Mangiafico S. 2021 rcompanion: Functions to Support Extension Education Program Evaluation. R package version 2.4.1, **Vol. 10**, p. 146021.
50. Fox J, Monette G. 1992 Generalized collinearity diagnostics. *J. Am. Stat. Assoc.* **87**, 178–183. (doi:10.1080/01621459.1992.10475190)
51. Spiess AN. 2018 propagate: Propagation of Uncertainty. R package version 1.0-6. See https://cran.r-project.org/web/packages/propagate/propagate.pdf.
52. Ghoul M, Mitri S. 2016 The ecology and evolution of microbial competition. *Trends Microbiol.* **24**, 833–845. (doi:10.1016/j.tim.2016.06.011)
53. Oliveira NM, Niehus R, Foster KR. 2014 Evolutionary limits to cooperation in microbial communities. *Proc. Natl Acad. Sci. USA* **111**, 17 941–17 946. (doi:10.1073/pnas.1412673111)
54. Foster KR, Bell T. 2012 Competition, not cooperation, dominates interactions among culturable microbial species. *Curr. Biol.* **22**, 1845–1850. (doi:10.1016/j.cub.2012.08.005)
55. Frank SA. 1996 Models of parasite virulence. *Q. Rev. Biol.* **71**, 37–78. (doi:10.1086/419267)
56. Buckling A, Brockhurst MA. 2008 Kin selection and the evolution of virulence. *Heredity* **100**, 484–488. (doi:10.1038/sj.hdy.6801093)
57. Inglis RF, Gardner A, Cornelis P, Buckling A. 2009 Spite and virulence in the bacterium *Pseudomonas aeruginosa*. *Proc. Natl Acad. Sci. USA* **106**, 5703–5707. (doi:10.1073/pnas.0810850106)
58. West SA, Buckling A. 2003 Cooperation, virulence and siderophore production in bacterial parasites. *Proc. R. Soc. Lond. B* **270**, 37–44. (doi:10.1098/rspb.2002.2209)
59. Read AF, Taylor LH. 2001 The Ecology of Genetically Diverse Infections. *Science* **292**, 1099–1103. (doi:10.1126/science.1059410)
60. Granato ET, Ziegenhain C, Marvig RL, Kümmerli R. 2018 Low spatial structure and selection against secreted virulence factors attenuates pathogenicity in *Pseudomonas aeruginosa*. *ISME J.* **12**, 2907–2918. (doi:10.1038/s41396-018-0231-9)
61. Massey RC, Buckling A, Ffrench-Constant R. 2004 Interference competition and parasite virulence. *Proc. R. Soc. Lond. B* **271**, 785–788. (doi:10.1098/rspb.2004.2676)
62. Boots M, Mealor M. 2007 Local Interactions Select for Lower Pathogen Infectivity. *Science* **315**, 1284–1286. (doi:10.1126/science.1137126)
63. Schmitz DA, Allen RC, Kümmerli R. 2023 Data from: Negative interactions and virulence differences drive the dynamics in multispecies bacterial infections. Dryad, Dataset. (doi:10.5061/dryad.z08kprrjj)
64. Schmitz DA, Allen RC, Kümmerli R. 2023 Negative interactions and virulence differences drive the dynamics in multispecies bacterial infections. Figshare. (doi:10.6084/m9.figshare.c.6729983)